Heliyon 10 (2024) e24217

Contents lists available at ScienceDirect

Heliyon

journal homepage: www.cell.com/heliyon

Research article

Preparation and characterization of a nanohydroxyapatite and sodium fluoride loaded chitosan-based *in situ* forming gel for enamel biomineralization

Azade Rafiee [a], Negin Mozafari [b], Neda Fekri [c], Mahtab Memarpour [a], Amir Azadi [b,d,*]

[a] *Oral and Dental Disease Research Center, Department of Pediatric Dentistry, School of Dentistry, Shiraz University of Medical Sciences, Shiraz, Iran*
[b] *Department of Pharmaceutics, School of Pharmacy, Shiraz University of Medical Sciences, Shiraz, Iran*
[c] *Student Research Committee, School of Dentistry, Shiraz University of Medical Sciences, Shiraz, Iran*
[d] *Pharmaceutical Sciences Research Center, Shiraz University of Medical Sciences, Shiraz, Iran*

ARTICLE INFO

Keywords:
Dentistry
Biomimetic
Fluoride
Hydroxyapatites
In situ hydrogel
Poloxamer

ABSTRACT

The development of remineralizing smart biomaterials is a contemporary approach to caries prevention. The present study aimed at formulation preparation and characterization of a thermoresponsive oral gel based on poloxamer and chitosan loaded with sodium fluoride (NaF) and nanohydroxyapatite (nHA) to treat demineralization. The chemical structure and morphology of the formulation were characterized using FTIR and FESEM-EDS tests. Hydrogel texture, rheology, and stability were also examined. The hydrogel was in a sol state at room temperature and became gel after being placed at 37 °C with no significance different in gelation time with the formulation without nHA and NaF as observed by *t*-test. The FTIR spectrum of nHA/NaF/chitosan-based hydrogel indicated the formation of physical crosslinking without any chemical interactions between the hydrogel components. The FESEM-EDS results demonstrated the uniform distribution of each element within the hydrogel matrix, confirming the successful incorporation of nHA and NaF in the prepared gel. The hardness, hydrogel's adhesiveness, and cohesiveness were 0.9 mJ, 1.7 mJ, and 0.37, respectively, indicating gel stability and the acceptable retention time of hydrogels. The formulation exhibited a non-Newtonian shear-thinning pseudoplastic and thixotropic behavior with absolute physical stability. Within the limitation of in vitro studies, nHA/NaF/chitosan-based *in situ* forming gel demonstrated favorable properties, which could be trasnsorm into a gel state in oral cavity due to poloxamer and chitosan and can prevent dental caries due to nHA and NaF. We propose this formulation as a promising dental material in tooth surface remineralization.

1. Introduction

Dental caries is a multifactorial biofilm-mediated disease resulting in dental mineral loss and tooth structure deterioration. Recent strategy to control caries focuses on lesion progression inhibition and remineralization improvement with remineralizing agents [1]. Historically, fluoride has been the first attempt in dental practice for preventive purposes [2]. Fluoride ions interact with dental hydroxyapatite to form fluoridated hydroxyapatites or fluorapatites, which are more resistant to acid attacks [3]. Subsequently,

* Corresponding author. Department of Pharmaceutics, School of Pharmacy, Shiraz University of Medical Sciences, Shiraz, Iran.
E-mail address: aazadi@sums.ac.ir (A. Azadi).

https://doi.org/10.1016/j.heliyon.2024.e24217
Received 8 August 2023; Received in revised form 16 December 2023; Accepted 4 January 2024
Available online 7 January 2024

chitosan, bioactive glass-containing sodium phosphosilicate [4], sodium trimetaphosphate, biofilm modifiers (arginine, triclosan, and xylitol) [5], functionalized beta-tricalcium phosphate, and self-assembling peptides [6] were developed. Recently, casein phosphopeptide-amorphous calcium phosphate [7] and biomimetic nanohydroxyapatite (nHA) [8] have been introduced and showed promising results [9].

Professionally, sodium fluoride (NaF) is marketed as gel, foam, and varnish [10]. Fluoride varnish is superior to the gel form due to its prolonged contact time on the tooth surface, which prevents the immediate drop of fluoride concentration in the oral environment [11,12]. Although topical fluoride application increases the surface microhardness of the existing layer and reduces the apatite dissolution, its application cannot replace the lost mineral structure [13]. Hydroxyapatite is one of the most studied dental biomaterials due to its bioactivity, biocompatibility, and status as the primary mineral constituent of enamel, dentin, and bone. Unlike fluoride compounds, hydroxyapatite can remineralize the incipient caries lesion by a new synthetic enamel layer formation, forming a protective coating on dental surfaces [3,8,14].

Hydrogels have long been among the most studied materials for biomedical applications and local drug delivery [15]. *In situ*-forming gels have sol-to-gel transition behavior in response to physical or chemical stimuli such as light, temperature, mechanical force, UV irradiation, pH change, chemical agents, etc. [16]. The *in situ*-forming thermoresponsive hydrogel systems have shown low viscosity during application and gel transition upon the change in temperature at the administration site [16,17]. Poloxamer is a non-ionic surfactant with an amphiphilic tri-block structure, which is usually used in thermoresponsive formulations due to its thermosensitive properties [18]. Chitosan is a natural polysaccharide that is obtained from the deacetylation or alkaline hydrolysis of chitin. Chitosan has advantageous properties, including biocompatibility, biodegradability, non-toxicity, and stability, which make it a suitable candidate for *in situ*-forming gels [19]. In biomedical applications, chitosan-based *in situ* gelling systems are promising for drug delivery [16]. According to earlier investigations, chitosan has been mixed with various ingredients like silver nanoparticles [20], collagen [21], hydroxyapatite [22–24], and fluoride [12,25–27]. As an example, the incorporation of 10 wt.% nHA in a hybrid chitosan/gelatin scaffold loaded with dental pulp stem cells promoted biomineralization, and induced the formation of a nanocrystalline hydroxyapatite-rich dentin-like matrix [24].

Enamel biomineralization is still a crucial demand, and advantageous outcomes related to using nHA/NaF/chitosan-based *in situ* forming gel could be expected. To the best of our knowledge, there is no available data regarding the effect of NaF and nHA on the overall characteristics and properties of the chitosan-based hydrogel. Therefore, the current study's objective was to prepare and characterize the chitosan-based *in situ*-gel forming formulation loaded with NaF and nHA as a smart biomaterial system candidate for remineralization.

2. Materials and methods

Intermediate molecular weight chitosan (MMWC; 75–85% deacetylated, Sigma Aldrich, USA), tripolyphosphate (TPP) (Merck, Darmstadt, Germany), poloxamer 407 (Pluronic F- 127) (Sigma Aldrich, USA), glacial acetic acid (Merck, Darmstadt, Germany), and glycerophosphate disodium salt hydrate (Merck, Darmstadt, Germany), nHA (Sigma Aldrich, USA), and NaF powder (Solarbio®, China) were utilized to prepare the formulation.

2.1. Preparation of in situ gel-forming formulation

To prepare the *in situ*-forming gel formulation, a method work previously by our team was developed with some modifications [16, 28–30]. In brief, 1% w/v medium molecular weight chitosan was dispersed in 0.1 N acetic acid solution under magnetic stirring overnight at room temperature to ensure complete dissolution. Next, 22%w/v poloxamer 407 was added to the chitosan solution. One hour after the entire amount of the poloxamer was dissolved, 10% w/w nHA and 5% w/w NaF were added under stirring at 125 rpm. After that, the mixture was transferred to the ice bath and left to cool for around 30 min. Next, 0.5% w/v TPP and 14.5% w/v glycerophosphate disodium salt hydrate were added dropwise to the mixture. The dispersion was stirred continuously in the ice bath for 1 h. The sol-to-gel transition was confirmed at the transfer of the mixture to a water bath at 37 °C after about 30 s.

2.2. Physico-chemical characterization

The functional groups present in chitosan, nHA particles, NaF particles, poloxamer 407, and freeze-dried nHA/NaF/chitosan-based hydrogel were identified with the Fourier transform infrared spectroscopy (FTIR) (Bruker 70, Germany) and dried-KBr disk technique between 400 and 4000 cm^{-1} region and at scanning resolution of 4 cm^{-1} to evaluate probable interactions between primary materials. After the FTIR spectra collection, the numerical values were transferred to Microsoft Office Excel (Microsoft Corporation, Washington, USA) for graphical representation [19]. The morphological microstructure of the samples was evaluated using energy dispersive spectroscopy associated with field emission scanning electron microscope (FESEM-EDS) (MIRA3, TSCAN, Brno, Czech Republic) at an accelerating voltage of 15 kV, with a spot size of 2–3 nm, and at ×35,000, ×75,000, and ×150,000 magnifications [19]. The samples were freeze-dried and sputter-coated with gold before FESEM-EDS characterization for 1 min at 20 mA. The values of calcium (Ca), phosphorus (P), sodium (Na), fluorine (F), carbon (C), and oxygen (O) content in weight (wt.%) were recorded by EDS at a beam voltage of 15 kV at a working distance of 25 mm. The EDS-elemental mapping was also performed to visualize the distribution of each element in the specimen.

2.3. Texture analysis and rheological properties

The texture of the hydrogels in the gel state was assessed using a texture analyzer device (TexturePro CT V1.5 Build, Brookfield, UK). The hydrogels were compressed by lowering the probe of the texture analyzer at a test speed of 1 cm/s and trigger load of 10 g. The force-displacement data during the compression test were obtained, and the texture parameters such as hardness, cohesiveness, and adhesiveness were calculated by TexturePro CT software (TexturePro CT software, Brookfield, UK).

One millimeter of hydrogel was used to measure the hydrogel viscosity and its behavior under different stresses using a cone/plate rheometer (DVNext Wells, Brookfield, UK) with 1 mm gap distance at 0.2 % strain and angular frequency of 1 rad s−1 at 25 °C. As the rheometer cone rotated the hydrogel surface, the torque, which is proportional to the resistance of the hydrogel to deformation, and the angular velocity of the cone, which is the deformation rate, were measured. The recorded data were used to calculate the viscosity of the hydrogel, and the numerical values were transferred to Microsoft Office Excel (Microsoft Corporation, Washington, USA) for graphical representation [31].

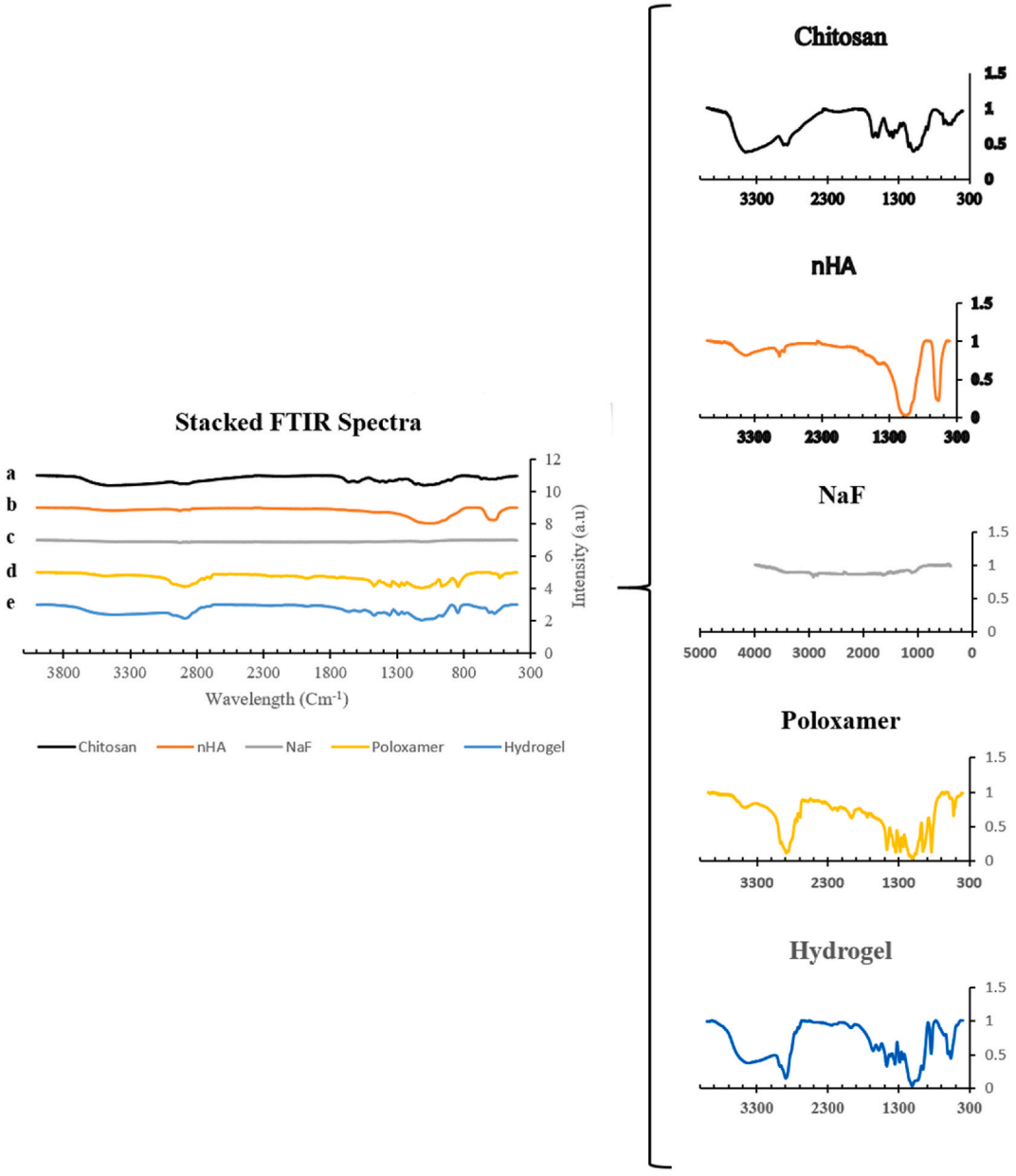

Fig. 1. The FTIR spectrum of chitosan, nHA particles, NaF particles, poloxamer 407, and freeze-dried nHA/NaF/chitosan-based hydrogel. a) chitosan, b) nHA particles, c) NaF particles, d) poloxamer 407, and e) freeze-dried nHA/NaF/chitosan-based hydrogel.

2.4. Thermo-responsive behavior and physical stability evaluation

The gel transition ability of the sol form after 1, 3, 7, 14, 21, 30, 60, and 90 days of keeping in the fridge (2–8 °C) was evaluated. At each period, the sol form was monitored visually for changes in physical properties, such as color, texture, phase separation, particle settling, and gelation. Besides, the sol-to-gel transition time was measured. During each interval, the gel state was centrifuged at 1000, 2000, 3000, and 4000 rpm for 10 min to assess any signs of physical instability, such as phase separation, sedimentation, or collapse [16].

2.5. Data presentation

All assays were performed in three technical replicates each (n = 3), and unpaired *t*-test was performed to investigate the significance. The compatible software generated the data for each test.

3. Results

3.1. Preparation of in situ gel-forming formulation

The in-situ gel forming hydrogel was formulated with various variables to find out an optimum condition in which the formulation turns into a gel state in less than 1 min at 37 °C. The gelation time of the optimum formulation was 29.33 ± 1.15 s, which showed that adding nHA and NaF had insignificant effect (*P value > 0.05)* on gelation time.

3.2. Physico-chemical characterization

The stacked FTIR spectrum of chitosan, nHA particles, NaF particles, poloxamer 407, and freeze-dried nHA/NaF/chitosan-based hydrogel are illustrated in Fig. 1a–e. The obtained spectrum of chitosan showed characteristic functional groups (Fig. 1a). A broad band at 3455 cm^{-1} indicates N–H group vibration stretching, O–H group vibration, and intramolecular hydrogen bonds. The 2920 and 2880 cm^{-1} peaks correspond to C–H symmetric and asymmetric stretching, respectively. The bands for C=O stretching of amide I at 1660 cm^{-1} and for C–N stretching of amide III at 1382 cm^{-1} confirm the presence of residual *N*-acetyl groups. The small band at 1590 cm^{-1} corresponds to the N–H bending of amide I. A peak at 1458 cm^{-1} indicates CH_2 bending and a peak at 1375 cm^{-1} represents CH3 symmetrical deformations. The signals at 1260 cm^{-1} and 1242 cm^{-1} confirm the O–H bending vibration and stretching vibration for N–C–O, respectively. The C–O–C bridge vibration stretching is noticed at 1068 cm^{-1} and 1030 cm^{-1}. The peak at 900 cm^{-1} is attributed to the CH bending out of the plane of the ring of monosaccharides. The FTIR spectrum of nHA is illustrated in Fig. 1b. A wide band, from 2800 cm^{-1} to 3600 cm^{-1}, with a peak at 3450 cm^{-1} and 2925 cm^{-1}, is attributed to the OH group stretching vibration. Apatitic PO_4^{3-} vibration forms an infrared absorption band at 1057 cm^{-1} (P–O asymmetric stretching vibration) and 569 cm^{-1}(P–O asymmetric bending vibration). The FTIR spectrum of NaF, as shown in Fig. 1c, demonstrates a peak at 2930 cm^{-1} due to water adsorption (OH group stretching vibration). A weak peak at 1120 cm^{-1} indicates the presence of monofluoride in the structure. The principal infrared absorption peaks of poloxamer 407 are demonstrated in Fig. 1d. The signal at 2888 cm^{-1} corresponds to aliphatic C–H stretching. A peak at 1345 cm^{-1} and 1111 cm^{-1} is attributed to in-plane O–H bending and C–O stretching, respectively. The IR spectrum of nHA/NaF/chitosan-based hydrogel, as shown in Fig. 1e, displayed a superimposed pattern of the minerals, chitosan, and poloxamer peaks with slight shifting of the peaks. The FTIR spectrum of freeze-dried nHA/NaF/chitosan-based hydrogel exhibited no

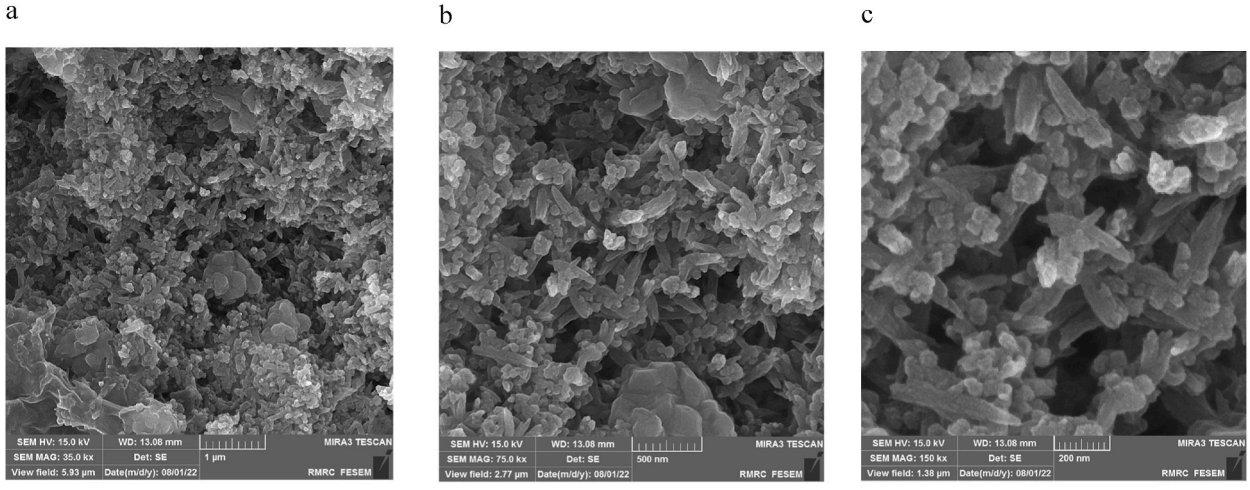

Fig. 2. The SEM image of nHA/NaF/chitosan-based hydrogel at a) ×35,000, b) ×75,000, and c) ×150,000 magnification.

dramatic differences compared to the FTIR spectra of chitosan and poloxamer (Fig. 1e).

The microstructure of nHA/NaF/chitosan-based hydrogel at different magnifications is illustrated in Fig. 2a–c. The FESEM images demonstrated the mineral islands within the three-dimensional hydrogel structure. The rod-like crystals of nHA form a network inside the pores of the chitosan matrix. The characteristic peaks of Ca, P, Na, F, C, and O elements were detected with EDS analysis (Fig. 3). The values of elemental composition in weight (wt.%) are presented in Table 1. The nHA/NaF/chitosan-based hydrogel had a Ca/P ratio of 1.51. The EDS-elemental mapping revealed the distribution of each element within the hydrogel matrix (Fig. 4a–g).

3.3. Texture analysis and rheological properties

The mechanical properties of *in situ* gel forming was evaluated by texture analysis. These properties are investigated to get information about gel stability and the retention time of *in situ* gel forming on the site of action [32]. Hardness represents the most force needed to deform the gel, adhesiveness is a force between the surface of the probe and the surface of the formulation, and cohesiveness is a work needed to deform the gel. The hydrogel's hardness, adhesiveness, and cohesiveness were 0.9 mJ, 1.7 mJ, and 0.37, respectively [33].

The Rheogram of the nHA/NaF/chitosan-based hydrogel has been demonstrated in Fig. 5a and b. The viscosity of the hydrogel was assessed as a function of shear stress (Pa) and shear rate (1/s) (Fig. 5a). The plastic viscosity of the hydrogel was 2.91 Pa. s. As evident in Fig. 5a, the rheogram has started from the rheogram's origin, and the downcurve is left to the upcurve. Therefore, the nHA/NaF/chitosan-based hydrogel has represented pseudoplastic-thixotropic behavior. Like formulations with non-Newtonian behavior, the prepared hydrogel did not have a constant viscosity (Fig. 5b). At lower shear rate, the prepared hydrogel represented high amount of viscosity and behaved like a solid. As the shear stress and subsequently, shear rate increased, the viscosity decreased quickly. The reverse phenomena happened when the stress was slowly removed. In other words, the hydrogel's viscosity decreased when the shear stress reduced at a constant shear rate, and the viscosity of the hydrogel recovered gradually.

3.4. Thermo-responsive behavior and physical stability evaluation

The sol-to-gel transition time remained approximately 30 s within three months of storage in the fridge at 2–8 °C. Besides, the gel form demonstrated physical stability under shearing stress for 10 min. The gel form did not separate into two phases during centrifugation at 1000–4000 rpm.

4. Discussion

The present study aimed to formulate and characterize a chitosan-based *in situ* gel-forming hydrogel loaded with NaF and nHA by focusing on the clinical translation of remineralizing smart biomaterial systems. The molecular weight and the degree of deacetylation (DD) can influence the chitosan properties [34]. Hydrophilicity and biocompatibility are positively correlated with DD, while degradation rate and viscosity are affected by molecular weight [34]. Therefore, chitosan with higher DD and medium molecular weight (to avoid excessive solution viscosity) is routinely employed for biomedical applications [34]. We used 1% w/v medium molecular weight chitosan (MMWC) with 75–85% degree of deacetylation. Chitosan, as one of the main components of the prepared formulation, is a unique biopolymer with a positive charge. Therefore, it can adhere to negatively charged surfaces, including dental enamel [35]. Besides, chitosan can adhere to the phosphate group of nHA and TPP and the fluoride ion of NaF in hydrogel via

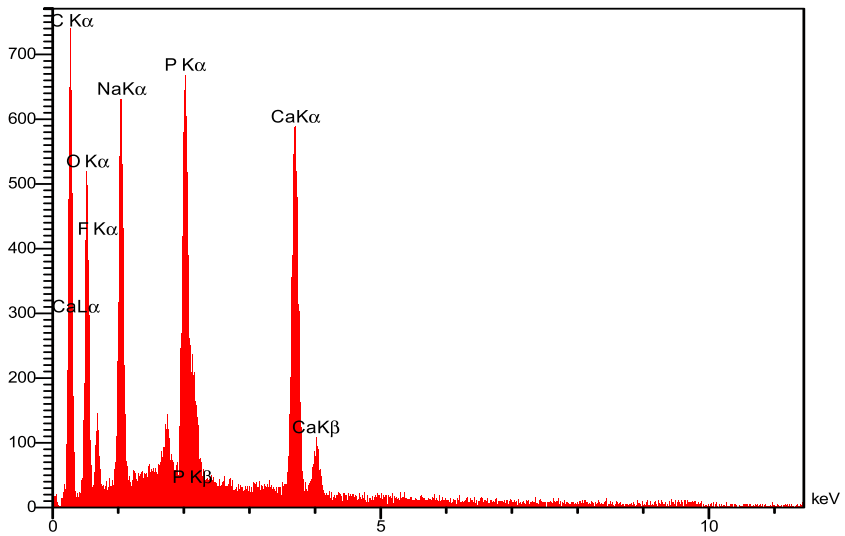

Fig. 3. The characteristic peaks of Ca, P, Na, F, C, and O elements detected with EDS analysis.

Table 1
The values of elemental composition in weight (wt.%).

Element	Wt.%
C	46.02
O	28.22
F	4.67
Na	6.46
P	5.82
Ca	8.80
Total	100.00

electrostatic forces [34]. Therefore, this hybrid hydrogel can entrap high concentrations of calcium, phosphate, and fluoride ions as the key remineralizing element, which is in line with the results of EDS-elemental mapping (Fig. 4a–g). It should be kept in mind that the hybrid hydrogel's inorganic and organic components might produce new characteristics in addition to their main properties [26]. The optimized formulation contained 5% w/w NaF and 10% w/w nHA. Fluoride varnishes contain 5% NaF and provide a high concentration of fluoride ions (22,600 ppm) during fluoride therapy [16]. It is claimed that a 0.1 ppm fluoride level in saliva is sufficient to provide anticaries effects [36]. According to Vagropoulou et al., incorporating 10% nHA in hybrid hydrogels could induce the formation of a nanocrystalline hydroxyapatite-rich dentin-like matrix and promote biomineralization [24]. Although higher concentrations of minerals seem favorable, higher concentrations of nHA in the optimized formulation resulted in the nHA particle agglomeration and the mechanical properties deterioration. The FTIR spectrum of freeze-dried nHA/NaF/chitosan-based hydrogel revealed a smoothened and superimposed pattern of nHA, NaF, Poloxamer, and chitosan peaks with no dramatic differences (Fig. 1e), indicating the presences of strong physical crosslinking mode interactions of the hydrogel components. The absence of a new characteristic peak in the hydrogel formulation revealed no chemical interaction between the organic and inorganic parts of the hydrogel [16]. nHA, NaF, and the freeze-dried nHA/NaF/chitosan-based gel demonstrated OH group stretching vibration at 2900 cm^{-1} to 2930 cm^{-1} due to water adsorption. The formation of hydrogen bonds between the minerals and the organic components is suggestive of the hydrophilic nature of the formulation. Although the hydrophilicity of the mixture can negatively affect the mechanical properties, it can positively influence the mucoadhesion and diffusion of body fluids and nutrients [19].

FESEM, as compared with SEM, provides more detailed microstructural data with higher resolution and less electrostatically-induced image distortion [37]. The FESEM image of the nHA/NaF/chitosan-based hydrogel demonstrated a homogenous distribution of the minerals in the chitosan hydrogel (Fig. 2a–c). The entrapped nHA particles exhibited nearly a uniform rod-like structure. It is claimed that the rod-like crystals of nHA positively affect the structure's mechanical properties [19]. We also employed the EDS analysis to determine the formulated hydrogel's Ca, P, Na, F, C, and O content. C and O elements are present in the chemical formula of chitosan ($C_{56}H_{103}N_9O_{39}$), poloxamer 407 ($C_{572}H_{1146}O_{259}$), glacial acetic acid (CH_3COOH), glycerophosphate disodium salt hydrate (C3H9Na2O7P), and TPP (Na5P3O10). P element is present in the chemical structure of TPP (Na5P3O10), glycerophosphate disodium salt hydrate (C3H9Na2O7P), and nHA (Ca5(PO4)3(OH)). Glycerophosphate disodium salt hydrate (C3H9Na2O7P) and sodium fluoride (NaF) contain Na element in their chemical composition. F and Ca elements are only present in the chemical structure of nHA (Ca5(PO4)3(OH)) and sodium fluoride (NaF), respectively. Therefore, the presence of Ca and F peaks in the EDS analysis of the hydrogel confirmed that nHA and NaF were successfully loaded in the prepared gel (Fig. 3). The hydrogel had a Ca/P ratio of 1.51, which is very close to the Ca/P ratio of nHA (1.67) (Table 1). The slight difference in the Ca/P ratio of the hydrogel and nHA is that, in addition to nHA, the P element is also present in the composition of glycerophosphate disodium salt hydrate and TPP. EDS-elemental mapping confirmed each element's uniform and desirable distribution of inside the gel matrix (Fig. 4).

The hydrogel's response to an external force during the texture analysis test provides reliable information about the mechanical properties of the semi-solid preparations, such as the ease of removal from the container, the spreadability of the product on the application site, and the bioadhessiveness [38]. In the present study, the hydrogel's hardness, adhesiveness, and cohesiveness were 0.9 mJ, 1.7 mJ, and 0.37, respectively. The maximum force recorded as the probe of the texture analyzer penetrates the hydrogel indicates hydrogel hardness. The hardness value of a hydrogel has a positive correlation with its consistency and density [32]. The lower the hardness values, the easier the hydrogel is removed from the container and applied on the application site [32]. Based on the hardness value, our prepared hydrogel showed an acceptable balance between consistency and ease of application. As the test probe of the texture analyzer moves upward (negative force), the adhesiveness and cohesiveness values of the hydrogel are measured. The more mechanical work required to remove the test probe from the gel, the more adhesive the sample is at the administration site [38]. Cohesiveness is defined as the maximum negative force measured during the upward motion of the test probe. The samples with higher cohesiveness values can restore their structure after application [32]. It is worth noting that the textural properties of a formulation are closely correlated with hydrogel component concentration [32]. According to Sezar et al., the chitosan concentration is positively correlated with gel adhesiveness but negatively correlated with gel cohesiveness [39]. Besides, higher concentrations of chitosan result in a more viscose NaF varnish [12]. Previous studies showed that the overall morphology, mechanical, and biological characteristics of electrospun chitosan nanofibers were not influenced by the incorporation of 0.5% wt.% nHA [22]. Also, adding 1–5 wt.% of hydroxyapatite to chitosan solution slightly improved the mechanical properties [23]. Our prepared chitosan-based hydrogel demonstrated satisfactory adhesiveness and cohesiveness values.

The hydrogel demonstrated a non-Newtonian shear-thinning pseudoplastic behavior (Fig. 5a). A positive correlation between the viscosity of the NaF varnish and chitosan concentration was reported previously [12]. The formulated hydrogel demonstrated a

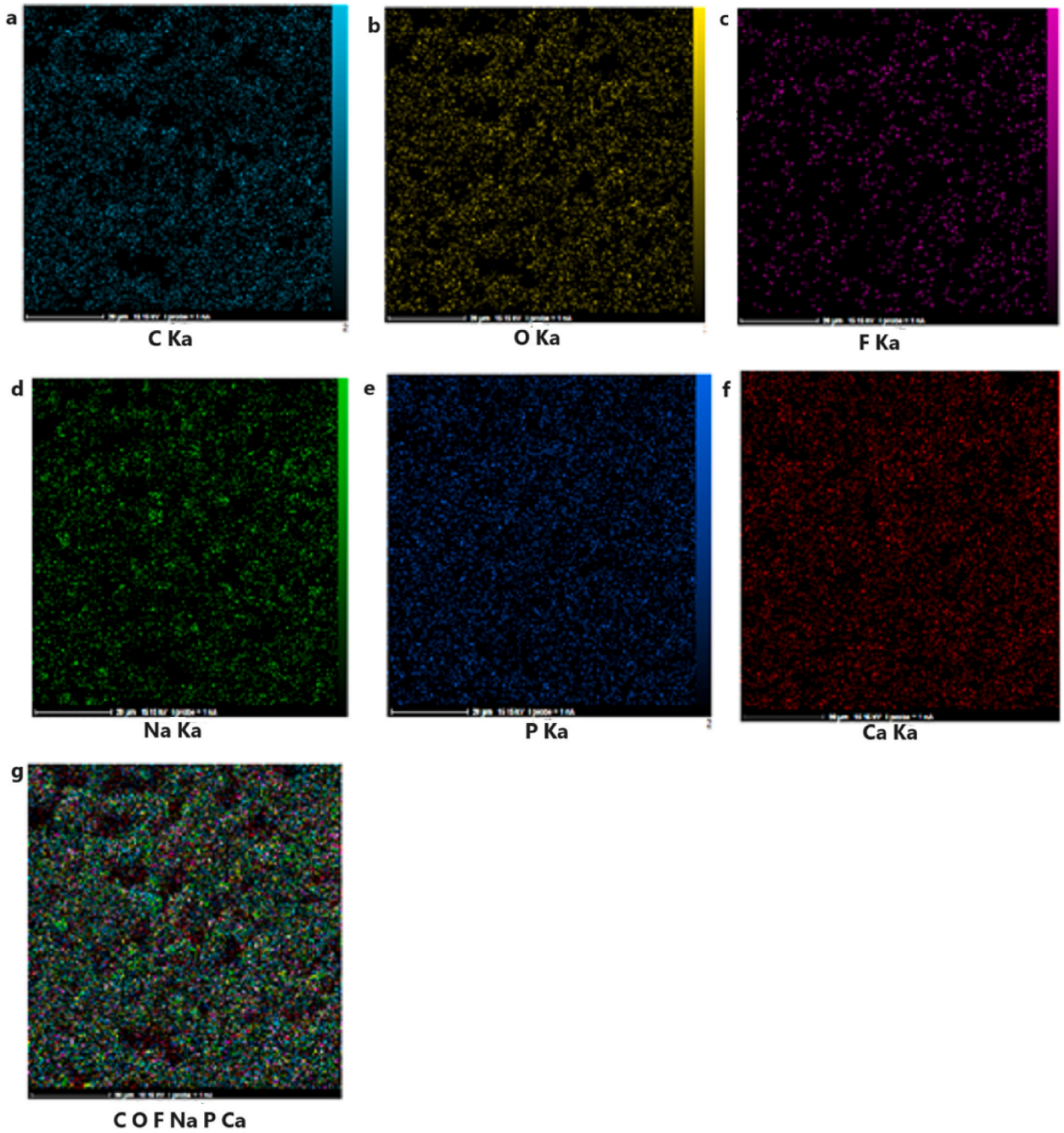

Fig. 4. The EDS-elemental mapping of elemental composition.

thixotropic behavior. The viscosity of a thixotropic material decreases over time at a constant shear rate and progressively restores when the shear stress stops [38]. Thixotropic behavior is a desirable characteristic of a topical hydrogel. This behavior implies that the hydrogel is initially thick, becomes thinner and spreadable under shear stress, and restores its viscosity once shear stress terminates, which increases its durability on the application site [35].

In addition to the easy-application characteristics of a hydrogel formulation, its physical stability at the application site and the container over a longer period is essential. Not only the prepared hydrogel was able to change from sol state (during storage in the fridge) into gel state (at 37 °C) in 30 s, but also this property was maintained over 90 days, which is an appropriate property in terms of clinical application. The gel's physical stability was confirmed as the gel form did not separate into two phases under shearing stress for 10 min.

Adding nHA and NaF was mainly due to their anticaries properties. Noteworthy, the addition of TPP and nHA has been reported to

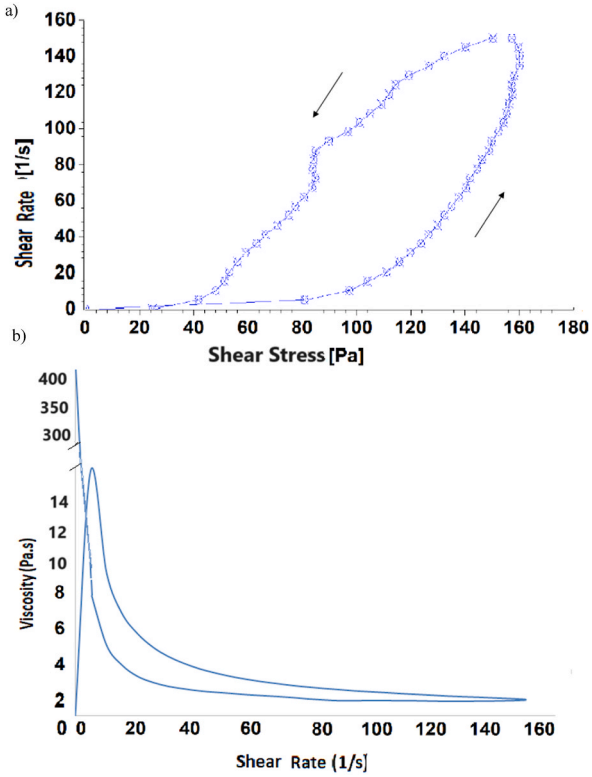

Fig. 5. a) shear stress (Pa)-shear rate (s-1) diagram of the nHA/NaF/chitosan-based hydrogel. b) viscosity (Pa.s)-shear rate (s-1) diagram of the nHA/NaF/chitosan-based hydrogel.

correlate with better mechanical properties [19,24,34,35]. Despite the hydrophilic nature of the synthesized gel, the prepared formulation revealed ideal mechanical characteristics. The improvement of mechanical properties might be attributed to the optimized formulation with suitable inorganic/organic ratio, formation of hydrogen bonds between the minerals and the organic components, incorporation of the TPP, and addition of rod-like nHA particles as inorganic reinforcement phase, which can occupy the porosities within the hydrogel structure [19]. NaF is an inorganic compound with low molecular weight (41.99 g/mol) and high water solubility (4.3 g/100 ml at 25 °C), which can assist the formation of nanoparticles by affecting the ionic strength of the solution [26]. Besides, F, the most reactive element in the periodic table, can actively bind to positive ions. This charge shielding effect provides an ideal medium for TPP to crosslink the chitosan chains resulting in a tighter matrix [26].

The prepared hydrogel formulation demonstrated properties that make it highly suitable for application during dental treatments. It had appropriate adhesiveness values, could be easily applied to the surface, and underwent a gelation process at body temperature, allowing it to conform to the shape of the tooth surface. The entrapment of fluoride and nHA inside the hydrogel can potentially lead to enhanced anticaries and remineralization effects. Overall, the optimized hydrogel formulation has potential applications in dental materials for caries prevention and remineralization therapy.

To our knowledge, this is the first study to formulate nHA/NaF/chitosan-based *in situ* forming gel. The absence of similar studies precluded appropriate comparisons. Within the limitation of the in vitro studies, our primary goal was to prepare and characterize the *in situ*-forming hydrogel. Theoretically, we propose that nHA/NaF/chitosan-based hydrogel can act as a biomineralizing agent due to the tight adsorption of chitosan to enamel, the chelating characteristic of amino groups in chitosan, and incorporation of nHA and NaF in the formulation. The present study has some limitations, including the evaluation of remineralization potential of the formulation, the release pattern of calcium, phosphate, and fluoride ions in the oral environment at different pH levels, the amount of mineral uptake and penetration into the sound and demineralized enamel surface, and the adhesiveness and retention time of formulation on the tooth surface.

5. Conclusion

A thermoresponsive nHA/NaF/chitosan-based *in situ*-forming gel was prepared by focusing on the clinical application of hydrogels in enamel biomineralization. The hydrogel was in a sol state at room temperature and became gel 30 s after placing it at body temperature. This characteristic remained constant during 90 days of the stability test. FTIR and FESEM-EDS analysis results confirmed the incorporation and uniform dispersion of calcium, phosphate, and fluoride into the chitosan matrix. The prepared chitosan-based hydrogel demonstrated acceptable consistency, hardness, adhesiveness, and cohesiveness values in texture analysis. Besides, the

hydrogel's shear-thinning, pseudoplastic, and thixotropic behavior highlighted that the formulation is injectable, spreadable, and retainable at the application site. The gel state demonstrated perfect physical stability under harsh centrifugation conditions. Further studies are recommended to assess the remineralization potential of the formulation, the release pattern of calcium, phosphate, and fluoride in the oral environment at different pH levels, the amount of mineral uptake and penetration into the sound and demineralized enamel surface, and the adhesiveness and retention time of formulation on the tooth surface.

Ethics approval

The study was approved by the Ethics Review Committee of the School of Dentistry, Shiraz University of Medical Sciences (IR.SUMS.DENTAL.REC.1400.118).

Data availability statement

The data that support the findings of this study are available from the corresponding author, Amir Azadi, upon reasonable request.

CRediT authorship contribution statement

Azade Rafiee: Writing – review & editing, Writing – original draft, Supervision, Software, Resources, Project administration, Funding acquisition, Formal analysis, Data curation, Conceptualization. **Negin Mozafari:** Writing – review & editing, Writing – original draft, Validation, Methodology, Formal analysis, Data curation, Conceptualization. **Neda Fekri:** Writing – original draft, Methodology, Investigation. **Mahtab Memarpour:** Writing – original draft, Visualization, Supervision, Project administration, Formal analysis. **Amir Azadi:** Writing – review & editing, Writing – original draft, Validation, Supervision, Resources, Project administration, Formal analysis, Data curation, Conceptualization.

Declaration of competing interest

The authors declare that they have no known competing financial interests or personal relationships that could have appeared to influence the work reported in this paper.

Acknowledgement

The authors thank the Vice-Chancellery of Research of Shiraz University of Medical Sciences, Shiraz, Iran, for supporting this research (Grant No. 24037). This article is based on thesis by Dr. Neda Fekri.

References

[1] A. Rafiee, M. Memarpour, H. Benam, Evaluation of bleaching agent effects on color and microhardness change of silver diamine fluoride-treated demineralized primary tooth enamel: an in vitro study, BMC Oral Health 22 (2022) 347.
[2] P. Zampetti, A. Scribante, Historical and bibliometric notes on the use of fluoride in caries prevention, Eur. J. Paediatr. Dent. 21 (2020) 148–152.
[3] A. Butera, M. Pascadopoli, S. Gallo, M. Lelli, F. Tarterini, F. Giglia, et al., SEM/EDS evaluation of the mineral deposition on a polymeric composite resin of a toothpaste containing biomimetic Zn-carbonate hydroxyapatite (microRepair®) in oral environment: a randomized clinical trial, Polymers 13 (2021) 2740.
[4] N. Kirthika, S. Vidhya, V. Sujatha, S. Mahalaxmi, R.S. Kumar, Comparative evaluation of compressive and flexural strength, fluoride release and bacterial adhesion of GIC modified with CPP-ACP, bioactive glass, chitosan and MDPB, J. Dent. Res. Dent. Clin. Dent. Prospects 15 (2021) 16.
[5] Y. Wang, J. Li, W. Sun, H. Li, R.D. Cannon, L. Mei, Effect of non-fluoride agents on the prevention of dental caries in primary dentition: a systematic review, PLoS One 12 (2017) e0182221.
[6] S.H. Kim, W. Hur, J.E. Kim, H.J. Min, S. Kim, H.S. Min, et al., Self-assembling peptide nanofibers coupled with neuropeptide substance P for bone tissue engineering, Tissue Eng. 21 (2015) 1237–1246.
[7] F. Fallahzadeh, S. Heidari, F. Najafi, M. Hajihasani, N. Noshiri, N.F. Nazari, et al., Efficacy of a novel bioactive glass-polymer composite for enamel remineralization following erosive challenge, Int. J. Dent. 2022 (2022).
[8] A. Butera, M. Pascadopoli, M. Pellegrini, B. Trapani, S. Gallo, M. Radu, et al., Biomimetic hydroxyapatite paste for molar–incisor hypomineralization: a randomized clinical trial, Oral Dis. (2022).
[9] P. Hemalatha, P. Padmanabhan, M. Muthalagu, M.S. Hameed, D.I. Rajkumar, M. Saranya, Comparative evaluation of qualitative and quantitative remineralization potential of four different remineralizing agents in enamel using energy-dispersive X-ray: an in vitro study, J. Conserv. Dent. JCD 23 (2020) 604.
[10] R.H. Selwitz, A.I. Ismail, N.B. Pitts, Dental caries, Lancet 369 (2007) 51–59.
[11] C. Chu, E. Lo, A review of sodium fluoride varnish, Gen. Dent. 54 (2006) 247–253.
[12] W. Pichaiaukrit, N. Thamrongananskul, K. Siralertmukul, S. Swasdison, Fluoride varnish containing chitosan demonstrated sustained fluoride release, Dent. Mater. J. 38 (2019) 1036–1042.
[13] J.S. Swarup, A. Rao, Enamel surface remineralization: using synthetic nanohydroxyapatite, Contemp. Clin. Dent. 3 (2012) 433.
[14] E. Pepla, L.K. Besharat, G. Palaia, G. Tenore, G. Migliau, Nano-hydroxyapatite and its applications in preventive, restorative and regenerative dentistry: a review of literature, Ann. Stomatol. 5 (2014) 108.
[15] F. Rizzo, N.S. Kehr, Recent advances in injectable hydrogels for controlled and local drug delivery, Adv. Healthcare Mater. 10 (2021) 2001341.
[16] M. Barati, S.M. Samani, L.P. Jahromi, H. Ashrafi, A. Azadi, Controlled-release in-situ gel forming formulation of tramadol containing chitosan-based pro-nanogels, Int. J. Biol. Macromol. 118 (2018) 1449–1454.
[17] B.V. Slaughter, S.S. Khurshid, O.Z. Fisher, A. Khademhosseini, N.A. Peppas, Hydrogels in regenerative medicine, Adv. Mater. 21 (2009) 3307–3329.
[18] M. Agrawal, S. Saraf, S. Saraf, S.K. Dubey, A. Puri, U. Gupta, et al., Stimuli-responsive in situ gelling system for nose-to-brain drug delivery, J. Contr. Release 327 (2020) 235–265.

[19] A.A. El-Fattah, A. Mansour, Viscoelasticity, mechanical properties, and in vitro biodegradation of injectable chitosan-poly (3-hydroxybutyrate-co-3-hydroxyvalerate)/nanohydroxyapatite composite hydrogel, Bull. Mater. Sci. 41 (2018) 1–10.
[20] Y. Liu, Y. Liu, N. Liao, F. Cui, M. Park, H.Y. Kim, Fabrication and durable antibacterial properties of electrospun chitosan nanofibers with silver nanoparticles, Int. J. Biol. Macromol. 79 (2015) 638–643.
[21] Z. Chen, P. Wang, B. Wei, X. Mo, F. Cui, Electrospun collagen–chitosan nanofiber: a biomimetic extracellular matrix for endothelial cell and smooth muscle cell, Acta Biomater. 6 (2010) 372–382.
[22] T.P. Sato, B.V. Rodrigues, D.C. Mello, E.A. Münchow, J.S. Ribeiro, J.P.B. Machado, et al., The role of nanohydroxyapatite on the morphological, physical, and biological properties of chitosan nanofibers, Clin. Oral Invest. 25 (2021) 3095–3103.
[23] E. Bulanov, N. Silina, M. Lelet, A. Knyazev, L. Smirnova, D. Aleynik, et al., Study of physicochemical properties of nanohydroxyapatite–chitosan composites, Bull. Mater. Sci. 43 (2020) 1–6.
[24] G. Vagropoulou, M. Trentsiou, A. Georgopoulou, E. Papachristou, O. Prymak, A. Kritis, et al., Hybrid chitosan/gelatin/nanohydroxyapatite scaffolds promote odontogenic differentiation of dental pulp stem cells and in vitro biomineralization, Dent. Mater. 37 (2021) e23–e36.
[25] G.M. Keegan, J.D. Smart, M.J. Ingram, L.M. Barnes, G.R. Burnett, G.D. Rees, Chitosan microparticles for the controlled delivery of fluoride, J. Dent. 40 (2012) 229–240.
[26] S. Nguyen, C. Escudero, N. Sediqi, G. Smistad, M. Hiorth, Fluoride loaded polymeric nanoparticles for dental delivery, Eur. J. Pharmaceut. Sci. 104 (2017) 326–334.
[27] H. Liu, B. Chen, Z. Mao, C. Gao, Chitosan nanoparticles for loading of toothpaste actives and adhesion on tooth analogs, J. Appl. Polym. Sci. 106 (2007) 4248–4256.
[28] M. Hamidi, A. Azadi, H. Ashrafi, P. Rafiei, S. Mohamadi-Samani, Taguchi orthogonal array design for the optimization of hydrogel nanoparticles for the intravenous delivery of small-molecule drugs, J. Appl. Polym. Sci. 126 (2012) 1714–1724.
[29] S. Jahanbekam, N. Mozafari, A. Bagheri-Alamooti, S. Mohammadi-Samani, S. Daneshamouz, R. Heidari, et al., Ultrasound-responsive hyaluronic acid hydrogel of hydrocortisone to treat osteoarthritis, Int. J. Biol. Macromol. 240 (2023) 124449.
[30] M. Hamidi, A. Azadi, S. Mohamadi-Samani, P. Rafiei, H. Ashrafi, Valproate-Loaded hydrogel nanoparticles: preparation and characterization, J. Appl. Polym. Sci. 124 (2012) 4686–4693.
[31] M. Samiei, E.D. Abdollahinia, N. Amiryaghoubi, M. Fathi, J. Barar, Y. Omidi, Injectable thermosensitive chitosan/gelatin hydrogel for dental pulp stem cells proliferation and differentiation, BioImpacts BI 13 (2023) 63.
[32] J. Hurler, A. Engesland, B. Poorahmary Kermany, N. Škalko-Basnet, Improved texture analysis for hydrogel characterization: gel cohesiveness, adhesiveness, and hardness, J. Appl. Polym. Sci. 125 (2012) 180–188.
[33] D.S. Jones, A.D. Woolfson, A.F. Brown, M.J. O'Neill, Mucoadhesive, syringeable drug delivery systems for controlled application of metronidazole to the periodontal pocket: in vitro release kinetics, syringeability, mechanical and mucoadhesive properties, J. Contr. Release 49 (1997) 71–79.
[34] X. Liu, Y. Wu, X. Zhao, Z. Wang, Fabrication and applications of bioactive chitosan-based organic-inorganic hybrid materials: a review, Carbohydr. Polym. 267 (2021) 118179.
[35] R.A. Hanafy, D. Mostafa, A. Abd El-Fattah, S. Kandil, Biomimetic chitosan against bioinspired nanohydroxyapatite for repairing enamel surfaces, Bioinspired, Biomimetic Nanobiomaterials 9 (2019) 85–94.
[36] J.D. Featherstone, Delivery challenges for fluoride, chlorhexidine and xylitol, in: BMC Oral Health, BioMed Central, 2006, pp. 1–5.
[37] M. Memarpour, F. Shafiei, A. Rafiee, M. Soltani, M.H. Dashti, Effect of hydroxyapatite nanoparticles on enamel remineralization and estimation of fissure sealant bond strength to remineralized tooth surfaces: an in vitro study, BMC Oral Health 19 (2019) 1–14.
[38] I.L. Dejeu, L.G. Vicaș, L.L. Vlaia, T. Jurca, M.E. Mureșan, A. Pallag, et al., Study for evaluation of hydrogels after the incorporation of liposomes embedded with caffeic acid, Pharmaceuticals 15 (2022) 175.
[39] A.D. Sezer, E. Cevher, F. Hatıpoğlu, Z. Oğurtan, A.L. Baş, J. Akbuğa, Preparation of fucoidan-chitosan hydrogel and its application as burn healing accelerator on rabbits, Biol. Pharm. Bull. 31 (2008) 2326–2333.